Research article

SURFACE and INTERFACE ANALYSIS

Received: 4 December 2012 Revised: 7 May 2013 Accepted: 12 May 2013 Published online in Wiley Online Library

(wileyonlinelibrary.com) DOI 10.1002/sia.5298

Surface modification of titanium by anodic oxidation in phosphoric acid at low potentials. Part 2. In vitro and in vivo study

A. Gomez Sanchez,[a]* W. Schreiner,[b] J. Ballarre,[a] A. Cisilino,[a] G. Duffó[c,d] and S. Ceré[a]

Electrochemical studies in SBF solution were performed, in order to determine the best corrosion resistance condition, comparing as-received titanium, covered with its native surface oxide, and titanium anodized in phosphoric acid. The results indicate that the anodic films obtained at a constant potential of 30 V have higher barrier effect, and the protective layer remains effective against the aggressive anions present in SBF after 30 days of immersion. Due to the promising corrosion performance in simulated biological media coupled with the biocompatible surface characteristics, anodic films on titanium obtained at 30 V were implanted on Wistar Rats to compare the osseointegration results of this modified surface with that corresponding to as-received titanium. It was found that, after 8 weeks of implantation, although the amount of bone surrounding the implant did not differ across the two different surface implants conditions, bone formation at the implant interface was found to be more homogeneous in anodized titanium.

Keywords: titanium; anodization; surface modification; in vivo implantation; tests in SBF

Introduction

Titanium and its alloys are the most extensively used metals in permanent implant applications due to its appropriate mechanical properties, corrosion resistance and biocompatibility.[1–3] Although as-received pure titanium have biocompatible characteristics and good corrosion resistance in biological media,[4,5] different surface modification routes have been developed to improve fixation of permanent implants to bone and also to diminish corrosion rate.[6–20] The requirement of excellent performance is mandatory specially when implantation occurs in young patients, in order to minimize replacement surgery.[21]

Although it is widely accepted that surface feature of permanent implant materials determines the rate and efficiency of the osseointegration process *in vivo*,[22–25] the phenomenon involved are still not fully understood, and therefore many efforts are focused on the effects of surface modification on osseointegration rate.[16,26–29] The correlation between the superficial features of the metallic materials used as surgical implants and the nucleation and growth processes that lead to osseointegration are a field of intense discussion due to the several unknown mechanisms involved with the event. Nowadays, the discussion about if the topographic features or the superficial chemistry are the responsible for the growth rate of calcium and phosphor compounds on the implants surface *in vitro* and i*n vivo* remains open.[23,30–35]

Histological evaluations that were carried out in different implant materials have proved that nanometer length scale modification effectively enhanced osseointegration,[36] but it is difficult to detect the effects of nano-scale modification with this technique. Therefore, for further understanding of these delicate alterations, a three-dimensional (3-D) evaluation using microcomputed tomography (micro-CT) can be used in order to investigate the unique surface modification at the nano-scale and correlate it with the bone formation and osseointegration.[37]

Once implanted, metals are in contact with extracellular fluids as blood and interstitial fluid. Chloride ion concentration in blood plasma is 113 mEq/l and in interstitial fluid is 117 mEq/l.[38] The human body acts, therefore, as a corrosive ambient for most metals, and requirements of degradation resistance are strong.[39] Increasing the thickness of surface oxide layer on titanium may be an efficient and non expensive route to increase corrosion resistance. However, porosity or non homogeneous film growth may occur in anodized films. Electrochemical tests in solutions with ion content similar to body fluids are useful to evaluate the barrier effect and stability of anodized valve metals.

In a previous work, titanium anodized in phosphoric acid at different potentials below 30 V was fully characterized.[40] The crystallographic phases present, the chemical elements incorporated during anodization, the electronic properties of surface

* *Correspondence to: A. Gomez Sanchez, INTEMA, Universidad Nacional del Mar del Plata - CONICET, Juan B. Justo 4302, (7600) Mar del Plata, Argentina E-mail: aaguar@gmail.com*

a *INTEMA, Universidad Nacional del Mar del Plata - CONICET, Juan B. Justo 4302, (7600) Mar del Plata, Argentina*

b *LSI – LANSEN, Departamento de Física, UFPR. Curitiba, Brazil*

c *Departamento de Materiales, Comisión Nacional de Energía Atómica – CONICET, Av. Gral. Paz 1499, (1650) San Martín, Buenos Aires, Argentina*

d *Universidad Nacional de Gral. San Martín, Av. Gral. Paz 1499, (1650) San Martín, Buenos Aires, Argentina*

films and the structure of the oxide layer were determined. It was found that the anodic oxide obtained by anodizing at 30 V presents biocompatible attributes: presence of anatase, incorporation of phosphor in the oxide layer and the electronic properties of the film correspond to those adequate to implant materials.[41]

With the aim of evaluating the corrosion resistance of the anodic films obtained on titanium, and together with the previous characterization, determining the best surface conditions for a permanent implant, electrochemical techniques including anodic polarization curves and electrochemical impedance spectroscopy (EIS), after 24 h and after 30 days immersion in simulated body fluid (SBF) solution, were performed.

Finally, the *in vivo* response of the as-received titanium and titanium anodized at 30 V were analyzed by 3-D imaging and bone quantification using micro-CT.

Experimental

Material and anodizing treatment

In vitro experiments were carried out using titanium grade 2 sheets (Roberto Cordes S.A., Argentina) from which 20 × 15 × 0.127 mm specimens were cut. The electrodes were anodized for 60 min in 1 mol/l H_3PO_4 at constant potentials between 3 and 30 V. The sample conditioning and oxide growth details were previously reported.[40,42]

Titanium grade 2 cylinders (Roberto Cordes S.A., Argentina) of 40–50 mm length and 0.8 mm diameter were used for the *in vivo* assays. As-received titanium and titanium anodized at constant potential of 30 V during 60 min in 1 mol/l H_3PO_4 were compared.

In a preliminary work, the reproducibility of the effect of anodizing of the two geometries of samples was evaluated by means of EIS in the anodizing solution.

SBF solution

Electrochemical and immersion tests were performed in a solution with ion concentration similar to blood plasma, which has been extensively used to evaluate the *in vitro* behavior of biomaterials.[43,44] All reagents were provided by Sigma-Aldrich (analytical grade, 85.0%), and deionized water (18.2 MΩ cm, Millipore) was used throughout. The solution was buffered to pH 7.4 with concentrated HCl and tris(hydroxymethyl)aminomethane (tris).

Titanium samples in the as-received condition and anodized at 30V were maintained in SBF following the recommendations of the ISO 23317:2007(E) standard.[45] The specimens were kept in SBF solution for 30 days at a constant temperature of 37 °C. The sample area (in mm^2) to the solution volume (in ml) ratio was set equal to 10.[46]

Electrochemical studies

Titanium electrodes in the as-received condition and anodized at different potentials were electrochemically studied in SBF using a conventional three-electrode cell with a saturated calomel electrode (Radiometer Analytical, France) as reference and a platinum wire as counter electrode. Measurements were performed after 24 h of immersion in SBF. Before each measurement, the potential was left for 40 min at open circuit potential. A Reference 600™ Potentiostat-Galvanostat-ZRA (Gamry Instruments, USA) was used and potentiodynamic polarization curves were measured from the open circuit potential to 1.5 V or until the current density reached a value of 10^{-2} A.cm^{-2}, and backwards at a sweep rate of 0.002 Vs^{-1}.

EIS measurements were carried out using a PCI4 750/potentiostat/galvanostat/ZRA™ (Gamry Instruments, USA). The amplitude of the perturbation signal was 10 mV rms, and the impedance was measured between 10^{-2} and 10^{6} Hz. The impedance data was fitted to equivalent circuit models with Zplot for Windows software.[47]

Anodic polarization and EIS measurements were repeated after 30 days of immersion in SBF for titanium in the as-received condition and anodized at 30 V.

In vivo experiments

Surgical procedure

In vivo experiments were conducted on four Wistar adult rats (weighted 350 ± 50 g), according to the codes and rules of the Interdisciplinary Bio-Ethics Programm University of Mar del Plata (April 2005). The surgical and preparation samples procedure was described before.[48,49] Briefly, the as-received and anodized Ti implants wires of 0.1 cm diameter and 3–4 cm length were sterilized in an autoclave for 20 min at 121 °C. Rats were anaesthetized with fentanyl citrate and droperidol according to their weight. Titanium samples corresponding to the as-received condition and anodized at 30 V were placed by press fit into the tibia, extending them into the medullar canal. Each animal had one 30 V anodized Ti implant in one leg and one as-received Ti sample in the opposite leg. The animals were sacrificed with an overdose of anesthesia after 60 days. Conventional X-ray radiographs were taken before retrieving the samples for control purposes. The bones with implants were ablated, cleaned from surrounding soft tissues and fixed in neutral 10 wt% formaldehyde for 24 h. Then, they were dehydrated in a series of ethanol–water mixture and finally embedded in methyl methacrylate (PMMA) solution and polymerized.

Micro-CT and 3D reconstructions

The 3D bone formation surrounding the implants was studied using micro-CT. The bone–implant PMMA embedded samples were imaged using a SkyScan 1172 (SkyScan, Kontich, Belgium) with an X-ray energy level of 100 KV and a current of 100 μA. Reconstructions were made using the software NRecon (SkyScan, Kontich, Belgium). The exam for as-received samples resulted in 980 micro-CT images of size 2000×2000 pixels with one-pixel separation. The resolution was 3.068 μm per pixel. Similarly, the scanning of the 30-V anodized samples resulted in 964 slices of size 2000×2000 pixels with one-pixel resolution. The resolution for this condition was 3.92 μm per pixel. The resulting reconstructed images were exported as grayscale BMP files.

The reconstructed images were processed for the removal of the ring artifact using the procedure due to Sijbers and Postnov.[50] This procedure consists in the transformation of the images into polar coordinates and the subtraction of the artifact template by means of a sliding-window filter. The procedure was coded using Matlab (MathWorks, Natick, MA, USA).

Cylindrical volumes of interest (VOI), coaxial with the implant axes, were used for the quantification of the bone volume. The radii of the VOIs were set equal to 675 μm; that means, 1.2 times the radio of the implant. Lengths of the VOIs were 3672 μm for the as-received titanium sample and 1900 μm for 30-V

anodized sample. The VOIs were constructed using the software DataViewer (Dataviewer V1.4.3; SkyScan, Kontich, Belgium) and an ad-hoc implemented Matlab subroutine. Figure 1 (a) illustrates a typical cross section of the VOI of the anodized sample.

Segmentation and quantification of the bone volume were performed using the program CTAn (CT Analyser V.10.1.3; SkyScan, Kontich, Belgium). The limit gray-shade values for the segmentation and quantification of the bone volume were selected as follows: The upper limit was set equal to that of the bone in contact with the implant. Due to the great contrast between the density (and the associated attenuation coefficients) of the bone and the implant material, this upper limit value is well marked, and it is easy to identify; hence, it was found not to be a source of error for the quantification of the bone volume. On the other hand, the lower limit, which indicates the border of the bone growth away from the implant, showed to be a sensitive parameter. Since the density of the bone is not homogeneous (especially for the newly grown bone), it is difficult to specify a single gray-shade value for the lower limit. Thus, the quantification of the bone volume was done using an average value for the lower limit, which was set after the best criterion of the analyst and then repeated using a variation of ±10% of the average value. The maximum change for each case was used as error indicator. The percentage of bone was calculated from the bone volume using the following formula:

$$B[\%] = \frac{bone\ volume \times 100}{VOI\ volume - implant\ volume} \quad (1)$$

Figure 1 (b) depicts an example of segmented cross sections. Finally, 3D reconstructions of the VOIs were prepared using CTAn and exported in STL format. The software MeshLab (MeshLab V1.3.0; Visual Computing Lab-ISTI-CNR; meshlab.sourceforge.net) was used for the visualization.

Results and discussion

Electrochcemical behavior of titanium in SBF

Anodic polarization curves

Anodic polarization curves of titanium as received and anodized at different potentials after 24 h immersion in SBF solution are presented in Fig. 2. In all conditions, the metal remains in the passive state during the test, as was previously reported.[51,52] A decrease of two orders of magnitude in the current density is observed between the as-received titanium and the anodized samples. The decrease in the current density corresponding to anodized titanium evidences an increase in the barrier affect of the anodic film compared with the native titanium oxide. This behavior is desired, but not always obtained with anodic growth of surface oxides. It has been demonstrated that when titanium and some of its alloys are anodized in sulfuric acid at the breakdown potential to enhance roughness, and thus promoting osseointegrable surfaces, the anodization process does not induce a reduction of current density.[53] This difference may be related to the conditions of growing of the surface oxides. When anodic oxides are grown at high potentials, near the rupture potential of the metal in the electrolyte, the corrosion resistance of the films is not obtained, due to the high porosity of the films. However, this is the surface modification usually performed when increase in the roughness is desired to increase bioactivity.[54] No major differences are evidenced among titanium anodized at increasing potentials between 3 and 30 V. This result may be related to the two-layered structure described by EIS in a previous work.[40] In this structure, the inner layer works as a barrier against aggressive ions, and the porous outer layer acts as an irregular surface with minor effect on corrosion resistance.

EIS

In Fig. 3, the EIS response of as-received and anodized titanium at different potentials is presented after 24 h of immersion in SBF solution. An increase of the total impedance of the system is observed when comparing titanium anodized at increasing

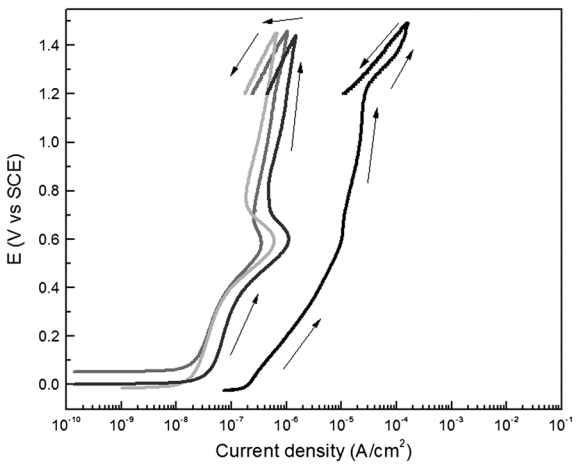

Figure 2. Anodic polarization curves of titanium as received (—) and anodized at 12 V (—) 24 V (—) and 30 V (—), after 24 h in SBF solution.

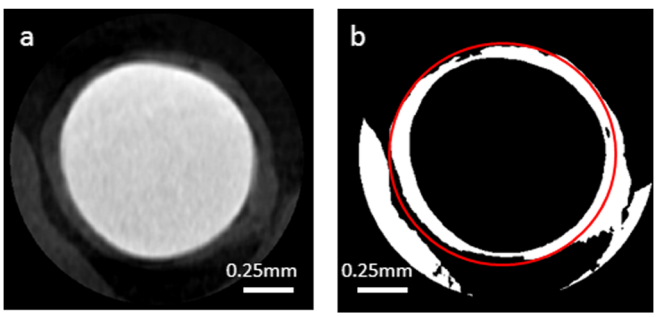

Figure 1. a. Annular cross section of the VOI used for the quantification of the bone surrounding the implant. b. Bone segmentation VOI cross section showing the area for bone measurement volume. The solid circle indicates the volume area limited for the analysis (1.2 times the radio of the implant).

potentials, along with the second time constant characteristic of a two-layer anodic film. The phase angle shifts to higher frequencies can be related to the thickening of the protective layer. The EIS response, along with the anodic polarization curves evidences an increases in the corrosion protection of the underlying metal when increasing the oxide film thickness.

The circuital models used to describe the EIS results obtained in SBF solution are presented in Fig. 4. The models are similar but not identical to those used in the electrochemical characterization of the films performed in the electrolyte used to perform the anodization,[40] due to the interactions between the metal/film system with the SBF solution.

The circuit (Fig. 4.a.), composed by a resistance (R) and a constant phase element (Q) in parallel with a resistance corresponding to the electrolyte (Re), led to an accurate fitting of the EIS results in SBF of as-received titanium. The constant phase element was used instead of an ideal capacitor to explain the deviations from a slope of −1 in the modulus Bode plot. The

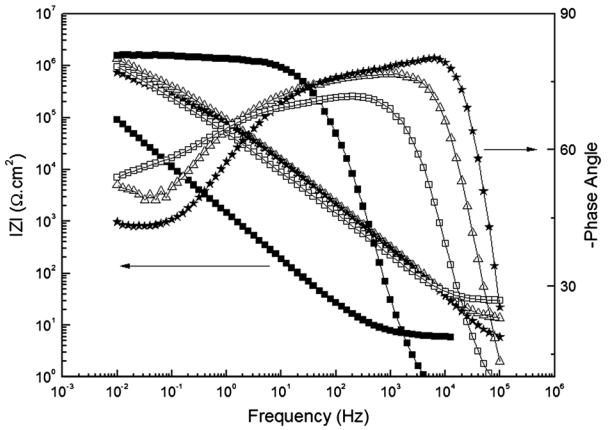

Figure 3. Bode plots after 24 h in SBF solution of (■) Ti as received, and anodized at: (□) 12 V, (Δ) 24 V, (*) 30 V. Solid line shows the equivalent circuit fitting.

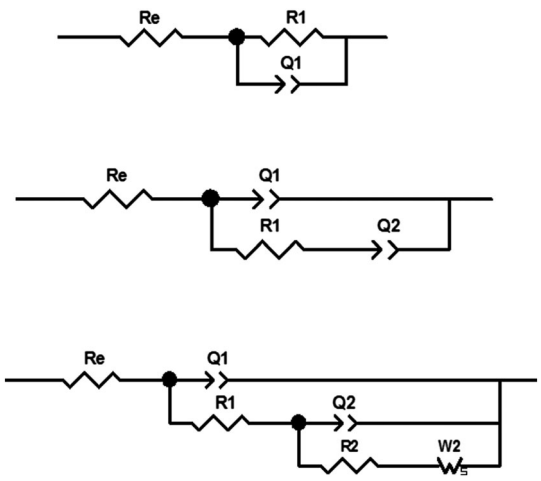

Figure 4. Equivalent circuits used to fit the data represented as solid lines in Figure 2. a. As-received titanium. b. Titanium anodized at 12 and 24 V. c. Titanium anodized at 30 V. In the circuits, Re corresponds to the solution resistance, R1 and Q1 correspond to the resistance and pseudocapacitance of the outer layer, R2 and Q2 the same meaning than above but for the inner layer and W2 corresponds to the Warburg impedance.

impedance of a constant phase element is characterized by two parameters: C is a parameter independent of frequency, and α is a coefficient associated with system homogeneity [83–88]. When $\alpha = 1$, C has units of capacitance ($F.cm^{-2}$) and represents the capacitance of the interface. When $\alpha < 1$, the system shows a behavior that can be attributed to surface heterogeneity or to a distribution of time constants, and, in this case, C has units of $s^{\alpha}.\Omega^{-1}.cm^{-2}$.

The circuit was previously used to fit EIS results of as-received titanium and some of its alloys in other SBF solutions.[19,55–58] However, other authors used double layer circuits to represent titanium and titanium alloys surfaces in phosphate buffer solutions or Hank's solution.[51,52,59,60] These solutions have similar ion concentration as the SBF; in particular, the chloride concentration and, therefore, titanium behavior may be similar in each of them. Thus, the main difference that leads to the different EIS response may be the surface finishing prior to the immersion and EIS test performing. In the cases mentioned above, all the samples were subjected to mechanical or electrochemical polish treatments, minutes prior immersion. Since metal surface features strongly influence the native oxide on valve metals, the surface finishing, with the corresponding removing of the native oxide, and rapid re-growth of the film may lead to a more porous or defective surface oxide. In this work, the native oxide represents the oxide growth after the lamination of the titanium sheets, when a high surface energy may lead to a dense native oxide.

Anodized samples are well represented by two-layered electrical models (Figs. 4.b. and 4.c.). These circuits represent an oxide structure composed by an inner (R2, Q2) compact layer in contact with the metal substrate and a porous outer layer in contact with the SBF solution (R1, Q1), where R and Q are the resistance and the constant phase element of the inner and outer layer. According to some authors, the open porosity found in anodic oxides leads to penetration of the electrolyte, with high interaction between the oxide layer and the electrolyte.[61]

For anodic films obtained at potentials below 12 V, EIS results are accurately fitted by the partially blocked electrode model represented in Fig. 4.b.[62] Samples anodized at higher voltages were modeled with the incorporation of a non faradaic resistance in the outer porous oxide layer, represented by a Warburg element (W_2, Fig. 4.c.). This circuital configuration describes the tortuosity or interconnectivity of the pores.[61]

Effective capacitance of anodic films obtained at various potentials on titanium is presented in Fig. 5. These values were calculated with the Brug equation.

$$C_{\text{eff}} = Q^{1/\alpha}\left(R_e^{-1} + R_t^{-1}\right)^{(1-\alpha)/\alpha} \quad (2)$$

In this equation, R_e is the electrolyte ohmic resistance, R_t relates to the charge transfer resistance associated with the kinetics of oxide growth and Q1 is the pseudocapacitance of the film.

The calculated values are in agreement with those reported for titanium alloys anodic films growth at potentials below 6 V in Hank solution.[63]

The decreasing of the effective capacitance when increasing anodizing potential is related to the increase of film thickness, and, in some cases, the thickness corresponding to each anodic growth condition may be estimated from EIS results.[40] However, in SBF, multiple possible interactions may be occurring between the electrolyte ions and the surface, leading to changes in

thickness during immersion (taken as the oxide with the penetrated solution, with possible precipitation of compounds on the surface, or adsorbed species, for instance). The impossibility to actually determine the surface state, and thus the corresponding permittivity of the layer, inhibits the estimation of the thickness of the film.

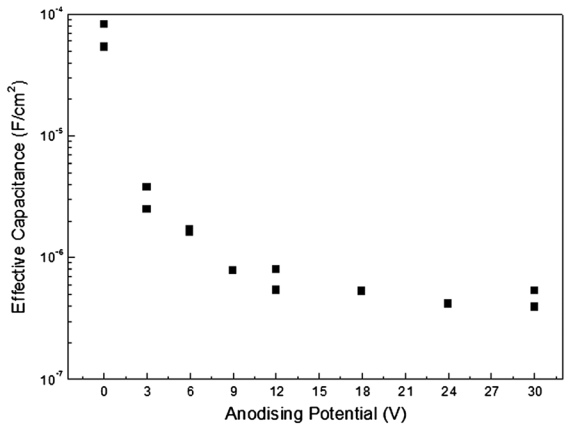

Figure 5. Effective capacitance of titanium anodized at different potentials corresponding to Eqn (2).

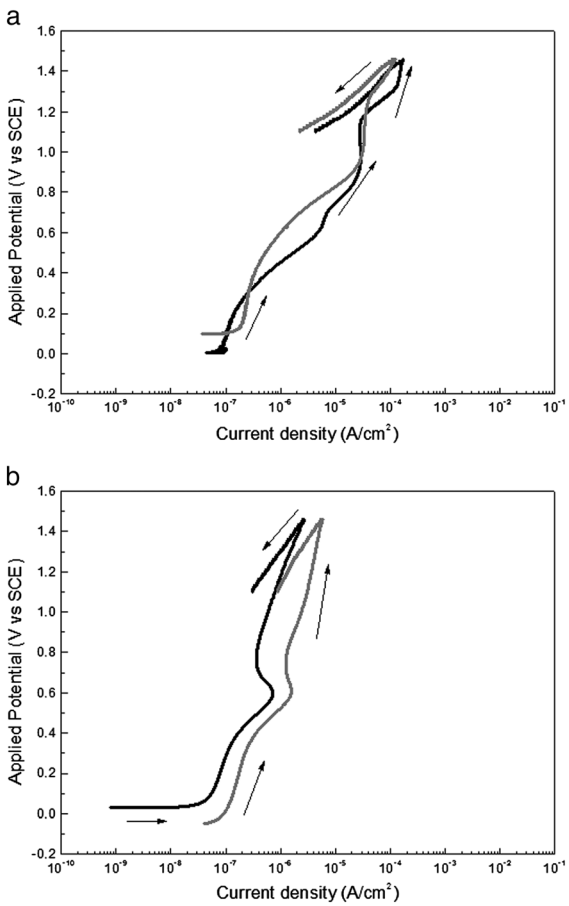

Figure 6. Anodic polarization curves of: a. As-received titanium after (—) 24 h and (—) 30 days of immersion in SBF solution. b. Titanium anodized at 30 V after (—) 24 h and (—) 30 days of immersion in SBF solution.

Electrochemical behavior of titanium in SBF after 30 days of immersion

Anodic polarization curves

In Fig. 6, the results of titanium as received (Fig. 6.a.) and anodized at 30 V (Fig. 6.b.) are compared after 24 h and 30 days of immersion in SBF at 37 °C. The prolonged immersion in SBF leads to a slight increase in the passivity current density on both conditions. These results evidence that the SBF exposition produces minor effects on both titanium surfaces, and the barrier layers remain effective against corrosion in SBF solution, since neither rupture of the film nor localized corrosion occurs.

EIS

No significant changes in corrosion barrier effect of the surface films (as received or anodized) are evidenced with EIS, in accordance with anodic polarization tests, as can be observed in Fig. 7. The stability of native oxide titanium surface in SBF was attributed to the adsorption of phosphates from the solution, with no further changes in the film structure or semiconducting properties,[64] and verified in Hank solution at different temperatures.[65] Anodic oxide films on titanium obtained in Ca and P containing media remain stable after 1000 h of immersion

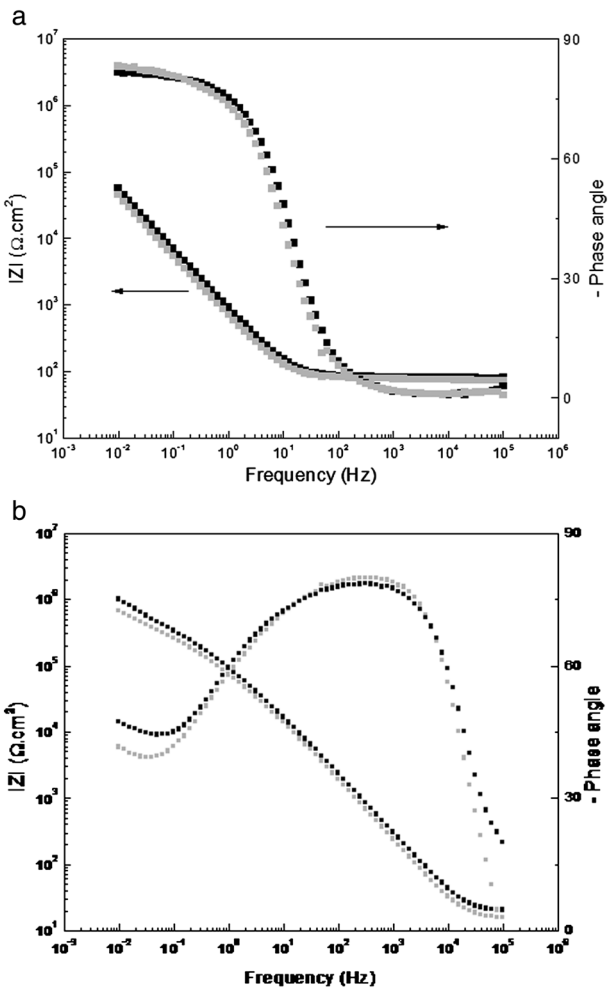

Figure 7. EIS results of: a. As-received titanium after (—) 24 h and (—) 30 days of immersion in SBF. b. Titanium anodized at 30 V after (—) 24 h and (—) 30 days of immersion in SBF.

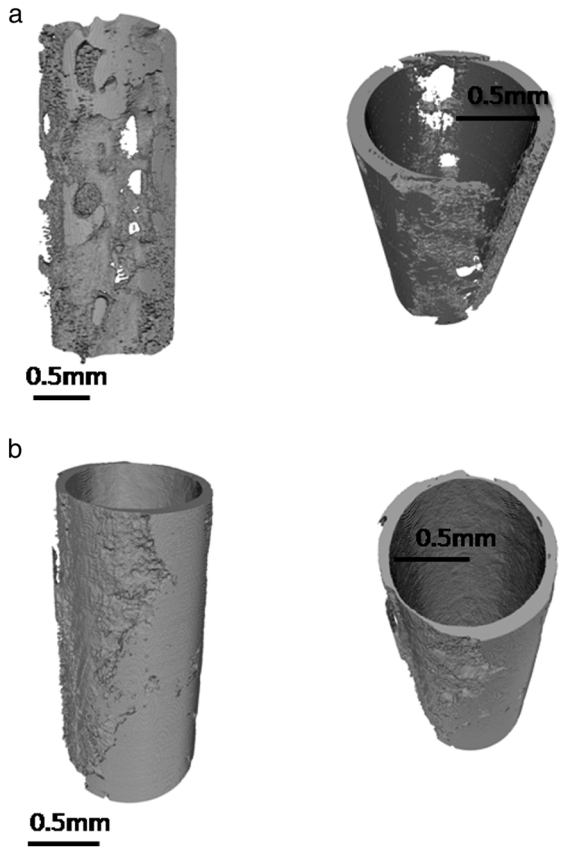

Figure 8. 3D reconstructions of the bone structure surrounding of: a. As-received titanium. b. Titanium anodized at 30 V implants. A superficial and a cross section are shown.

in SBF. However, such oxides did not present an increase in barrier effect compared to native oxides.[57]

When comparing the performance of as-received titanium with the anodized at 30 V, the increase of corrosion resistance obtained and the stability of the anodic film are presenting the anodized surface as the best candidate as a permanent implant. Moreover, as it was stated in the previous characterization of the surface, titanium anodized at 30 V presents biocompatible characteristics regarding the phosphate incorporation, the presence of anatase in the oxide and the number of carriers and therefore allows the expectation of a good in vivo performance.[40]

In vivo analysis: 3D micro-CT imaging

The 3D reconstructions of the bone structure surrounding the as-received and anodized implants are shown in Figs. 8.a. and 8.b., respectively. The percentage of bone surrounding the implants is 65.7 $\pm$7.5% for the as-received implant, and 62.9 $\pm$5.1% for the anodized implant. Although the bone volumes are similar for both implants, not showing any significant statistical difference, there is a marked difference between their topologies: while the bone around the anodized titanium (Fig. 8.b.) looks uniform and it completely covers the implant surface, the as-received titanium (Fig. 8.a.) presents uncovered portions around the implant surface. This technique is especially valuable when comparing the results of bone attachment measurement by histology images that measures contact area, since in micro-CT, the global process of osseointegration can be evaluated.[27,66–69] 3-D evaluation with micro-CT has received considerable attention in recent years because it facilitates the observation and quantification of bone formation surrounding implants or bone substitutes in a 3-D plane.[70–72]

Conclusions

The decrease in the current density corresponding to anodized titanium evidences an increase in the barrier affect of the anodic film compared with the native titanium oxide. Titanium anodized at different potentials from 3 to 30 V present similar barrier effect in SBF solution, as it was analysed by EIS and anodic polarization curves.

The prolonged immersion in SBF leads to a slight increase in the passivity current density in both the as-received and anodized condition. Although the results evidence that the SBF exposition produces minor effects on both titanium surfaces, the barrier layer remains effective against corrosion in SBF solution, since neither rupture of the film nor localized corrosion occurs.

When comparing the performance of as received with the anodized at 30 V titanium, the increase of corrosion resistance obtained, and the stability of the anodic film present the anodized surface as the best candidate as a permanent implant. Although the bone percentage does not greatly differ for both kinds of surfaces, there is a marked difference between their topologies: while the bone in the samples anodized at 30V looks uniform and completely covers the implant surface, as-received samples present uncovered portions of the implant surface.

References

[1] R. J. Solar, ASTM STP 684 **1979**, 259.
[2] P. Tengvall, I. Lundström, *Clinical Mat* **1992**, *9*, 115.
[3] S. G. Steinemann, *Periodontol. 2000* 2000 **1998**, *17*, 7.
[4] M. Navarro, A. Michiardi, O. Castaño, J. A. Planell, *J Royal Soc Interface* **2008**, *5*, 1137.
[5] M. Geetha, A. K. Singh, R. Asokamani, A. K. Gogia, *Prog Mat Sci* **2009**, *54*, 397.
[6] R. M. Souto, M. M. Laz, R. L. Reis, *Biomaterials* **2003**, *24*, 4213.
[7] C. Berbecaru, H. V. Alexandru, G. E. Stan, D. A. Marcov, I. Pasuk, A. Ianculescu, *Mat Sci Eng* **2010**, *B169*, 101.
[8] J.-H. Park, Y.-K. Lee, K.-M. Kim, K.-N. Kim, *Surf Coat Tech* **2005**, *195*, 252.
[9] P. Habibovic, F. Barrére, C.A. van Blitterswijk, K. de Groot, P. Layrolle, *J Am Cer Soc* **2002**, *85*, 517.
[10] J.-S. Oh, Y.-H. Lee, B.-A. Kang, S.-B. Kim, K.-S. Hwang, *Ceram Int* **2003**, *29*, 847.
[11] J. Faure, A. Balamurugan, H. Benhayoune, P. Torres, G. Balossier, J. M. F. Ferreira, *Mat Sci Eng* **2009**, *C29*, 1252–1257.
[12] M. Uchida, H.-M. Kim, F. Miyaji, T. Kokubo, T. Nakamura, *Biomaterials* **2002**, *23*, 313.
[13] J.-W. Park, Y.-J. Kim, J.-H. Jang, T.-G. Kwon, Y.-Ch. Bae, J.-Y. Suh, *Acta Biomater.* **2010**, *6*, 1661.
[14] M. Browne, P. J. Gregson, *Biomaterials* **2000**, *21*, 385–392.
[15] J. Hall, J. Lausmaa, *Appl Osseointegration Res.* **2000**, *1*, 1.
[16] Y.-T. Sul, C. B. Johansson, Y. Jeong, T. Albrektsson, *Med. Eng. Phys.* **2001**, *23*, 329.
[17] Y-T. Sul, C. B. Johansson, S. Petronis, A. Krozer, Y. Jeong, A. Wennerberg, T. Albrektsson, *Biomaterials* **2002**, *23*, 491.
[18] B. Yang, M. Uchida, H.-M. Kim, X. Zhang, T. Kokubo, *Biomaterials* **2004**, *25*, 1003.
[19] B. S. Ng, I. Annergren, A. M. Soutar, K. A. Khora, A. E. W. Jarfors, *Biomaterials* **2005**, *26*, 1087.
[20] X. Cui, H.-M. Kim, M. Kawashita, L. Wang, T. Xiong, T. Kokubo, T. Nakamura, *Dent. Mater.* **2009**, *25*, 80.
[21] Bone & Joint Decade's Musculoskeletal Portal **2007**, http://www.boneandjointdecade.org.

[22] G. Mendonca, D. B. S. Mendonca, F. J. L. Aragão, L. F. Cooper, *Biomaterials* **2008**, *29*, 3822.
[23] J. E. Davies, *Biomaterials* **2007**, *28*, 5058.
[24] A. L. Oliveira, J. F. Mano, R. L. Reis, *Curr Op Sol St Mat Sci* **2003**, *7*, 309.
[25] F. Barrere, M. M. E. Snel, C. A. van Blitterswijk, K. de Groot, P. Layrolle, *Biomaterials* **2004**, *25*, 2901.
[26] B. Yang, M. Uchida, H.-M. Kim, X. Zhang, T. Kokubo, *Biomaterials* **2004**, *25*, 1003.
[27] Y.-T. Sul, *Biomaterials* **2003**, *24*, 3893.
[28] W. Chrzanowski, J. Szewczenko, J. Tyrlik-Held, J. Marciniak, J. Zak, *J Mat Proc Tech* **2005**, *162–263*, 163.
[29] N. K. Kuromoto, R. A. Simão, G. A. Soares, *Mat Charac* **2007**, *58*, 114.
[30] C. Aparicio, F. J. Gil, C. Fonseca, M. Barbosa, J. A. Planell, *Biomaterials* **2003**, *24*, 263.
[31] J.-H. Lee, S.-E. Kim, Y.-J. Kim, Ch.-S. Chi, H.-J. Oh, *Mat Chem Phys* **2006**, *98*, 39.
[32] U. Joos, T. Wiesmann, T. Szuwart, U. Meyer, *Int J Oral Max Surg* **2006**, *35*, 783.
[33] L. Le Guéhennec, A. Soueidan, P. Layrolle, Y. Amouriq, *Dental Mat* **2007**, *23*, 844.
[34] C. Wirth, B. Grosgogeat, C. Lagneau, N. Jaffrezic–Renault, L. Ponsonet, *Mat Sci Eng C* **2008**, *28*, 990.
[35] V. Barranco, E. Onofre, M. L. Escudero, M. C. García–Alonso, *Surf Coat Tech* **2010**, *204*, 3783.
[36] B. H. Lee, C. Lee, D. G. Kim, K. Choi, K. H. Lee, Y. D. Kim, *Mat Sci Eng C* **2008**, *28*, 1448.
[37] P. G. Coelho, G. Giro, W. Kim, R. Granato, C. Marin, E. A. Bonfante, S. Bonfante, T. Lilin, M. Suzuki, *Oral Surg Oral Med O* **2012**, *114*, 437.
[38] T. Hanawa, *Mat Sci Eng A* **1999**, *267*, 260.
[39] N. T. C. Oliveira, S. R. Biaggio, S. Piazza, C. Sunseri, F. Di Quarto, *Electrochim. Acta* **2004**, *49*, 4563.
[40] A. Gomez Sanchez, W. Schreiner, G. Duffó, S. Ceré, *Surf. Interface Anal.* **2013**, *45*, 1037-1046.
[41] I. Petersson, J. E. L. Löberg, A. S. Fredriksson, E. K. Ahlberg, *Biomaterials* **2009**, *30*, 4471.
[42] A. Gomez Sanchez, W. Schreiner, G. Duffó, S. Ceré, *Appl. Surf. Sci.* **2011**, *257*, 6397.
[43] T. Kokubo, S. Ito, Z. T. Huang, T. Hayashi, S. Sakka, T. Kitsugi, T. Yamamuro, *J Biomed Mat Res* **1990**, *24*, 331.
[44] T. Kokubo, H. Kushitani, S. Sakka, *J Biomed Mat Res* **1990**, *24*, 721.
[45] International Standard ISO 23317:2007(E), **2007**.
[46] T. Kokubo, H. Takadama, *Biomaterials* **2006**, *27*, 2907.
[47] Zplot for Windows, Scribner Ass. Inc., Southern Pines, NC, **1998**.
[48] J. Ballarre, R. Seltzer, E. Mendoza, J. C. Orellano, Y. W. Mai, C. García, S. M. Ceré, *Mat Sci Eng C* **2011**, *31–3*, 545.
[49] J. Ballarre, I. Manjubala, W. H. Schreiner, J. C. Orellano, P. Fratzl, S. Ceré, *Acta Biomater.* **2010**, *6–4*, 1601.
[50] J. Sijbers, A. Postnov, *Phys. Med. Biol.* **2004**, *49*, 14.
[51] M. Aziz-Kerrzo, K. G. Conroy, A. M. Fenelon, S. T. Farell, C. B. Breslin, *Biomaterials* **2001**, *22*, 1531.
[52] N. Ibris, J. C. Mirza Rosca, *J.Electroanal. Chem.* **2002**, *526*, 53.
[53] H.-J. Song, M.-K. Kim, G.-Ch. Jung, M.-S. Vang, Y.-J. Park, *Surf Coat Tech* **2007**, *201*, 8738.
[54] H.-J. Song, S.-H. Park, S.-H. Jeong, Y.-J. Park, *J Mat Proc Tech* **2009**, *209*, 864.
[55] J. E. G. Gonzalez, J. C. Mirza-Rosca, *J.Electroanal. Chem.* **1999**, *471*, 109.
[56] M. V. Popa, I. Demetrescu, E. Vasilescu, P. Drob, A. S. Lopez, J. Mirza-Rosca, C. Vasilescu, D. Ionita, *Electrochim. Acta* **2004** ; *49* 2113.
[57] D. Krupa, J. Baszkiewicz, J. W. Sobczak, A. Bilinski, A. Barcz, *J Mat Proc Tech* **2003**, *143–144*, 158.
[58] M. E. P. Souza, L. Lima, C. R. P. Lima, C. A. C. Zavaglia, C. M. A. Freire, *J Mat Sci - Mater M* **2009**, *20*, 549.
[59] J. Pan, D. Thierry, C. Leygraf, *J Biomed Mat Res* **1994**, *28*, 113.
[60] J. Pan, D. Thierry, C. Leygraf, *Electrochim. Acta* **1996**, *41*, 1143.
[61] M. Metikos-Hukovic, Z. Grubac, *J.Electroanal. Chem.* **2003**, *556*, 167.
[62] M. Orazem, B. Tribollet, Electrochemical Impedance spectroscopy (ECS), T. Wiley, New York, **2008**.
[63] I. Milosev, T. Kosec, H.-H. Strehblow, *Electrochim. Acta* **2008**, *53*, 3547.
[64] A. W. E. Hodgson, Y. Muller, D. Forster, S. Virtanen, *Electrochim. Acta* **2002**, *47*, 1913.
[65] V. A. Alves, R. Q. Reis, I. C. B. Santos, D. G. Souza, T. F. de Gonçalves, M. A. Pereira-da-Silva, A. Rossi, L. A. da Silva, *Corros. Sci.* **2009**, *51*, 2473.
[66] M. Diefenbeck, T. MÃ¼ckley, C. Schrader, J. Schmidt, S. Zankovych, J. Bossert, K.D. Jandt, M. Faucon, U. Finger, *Biomaterials* **2011**, *32*, 8041.
[67] R. J. Kohal, M. Wolkewitz, M. Hinze, J. S. Han, M. BÃ¤chle, F. Butz, *Clin Oral Implan Res* **2009**, *20*, 333.
[68] C. Larsson, P. Thomsen, B. O. Aronsson, M. Rodahl, J. Lausmaa, B. Kasemo, L. E. Ericson, *Biomaterials* **1996**, *17*, 605.
[69] J. Xiao, H. Zhou, L. Zhao, Y. Sun, S. Guan, B. Liu, L. Kong, *Osteoporosis Int* **2011**, *22*, 1907.
[70] R. Jimbo, P. G. Coelho, S. Vandeweghe, H. O. Schwartz-Filho, M. Hayashi, D. Ono, M. Andersson, A. Wennerberg, *Acta Biomater.* **2011**, *7*, 4229.
[71] E. Baril, L. P. Lefebvre, S. A. Hacking, *J Mater Sci Materials in Medicine* **2011**, *22*, 1321.
[72] H. Sarve, J. Lindblad, G. Borgefors, C. B. Johansson, *Comput Meth Prog Bio* **2011**, *102*, 25.

